Collision Avoidance of Arbitrarily Shaped Deforming Objects Using Collision Cones

Vishwamithra Sunkara, Animesh Chakravarthy, and Debasish Ghose

***Abstract*—In this letter, the problem of collision avoidance of objects, which can deform by changing their shape as a function of time, is considered. There are several scenarios involving such deforming objects—examples include environments with shape-shifting robots, such as snake robots, boundaries of swarms of vehicles, and boundaries of oil spills. There is very limited work in the literature that considers dynamic environments comprising such shape changing entities. To develop conditions that predict the onset of collision for deformable objects, this letter uses the notion of collision cones in environments involving engagements between a point object and a deforming object, a circular object and a deforming object, and finally, an arbitrarily shaped object and a deforming object. The collision cone equations are subsequently embedded in a Lyapunov framework and used to develop nonlinear analytical guidance laws for collision avoidance in such environments. Simulations are performed to demonstrate the efficacy of the guidance laws.**

***Index Terms*—Collision avoidance, motion and path planning, deforming objects, collision cones.**

I. Introduction

REAL-TIME path planning of autonomous vehicles in rapidly changing environments still remains a challenge to the mobile robotics community. One of the reasons for an environment to change is linked to the unpredictable behavior of objects and other obstacles in the environment. Traditionally, such objects are considered to be non-deforming (that is, they retain the same size and shape over a reasonable period of time). However, there can be many instances of environments that contain deforming obstacles, whose shape changes with time. For example, an oil spill moving on an ocean surface changes its shape over time and represents a deforming obstacle to an autonomous boat attempting to navigate that environment. Other examples of deforming objects include shape changing robots (such as soft robotic systems like snake robots [1], [2]), robots carrying movable parts or manipulators, and a swarm of robotic vehicles considered as a single object. Few papers in the literature consider avoidance of such deforming obstacles. Exceptions are [3], where the problem of a moving and deforming obstacle is addressed using sliding mode control, [4]–[5], and [6] where path planning through deforming obstacles has been proposed using collision cones.

The concept of collision cones was proposed in [7] to represent a collection of velocity vectors of an object which leads to collision with another moving object. Guidance laws to avoid collision are then designed to pull the current velocity vector of the object outside the collision cone. This idea was later successfully exploited by many researchers for various applications ranging from automobile collision avoidance [8], aircraft conflict detection and resolution [9], vision based obstacle avoidance [10], robotic collision avoidance [11], and to study collision avoidance behavior in biological organisms [12]. The idea of collision cones was subsequently extended to higher dimensional spaces and general obstacle shapes [13]–[15] and also used to design safe passage trajectories through narrow orifices [16]. The collision cone concept has some relations with the maneuvering board approach [17], velocity obstacles [18], and forbidden velocity maps [19]. However, the collision cone approach is the only approach that explicitly considers arbitrarily shaped objects, which form an important aspect of deforming obstacles, unlike the others which consider only circular objects.

A general theory of avoiding deforming obstacles is not available in the literature. The paper [6] addresses an application of avoiding a deforming obstacle using radar measurement and the proposed collision cone based algorithm is very specific to that application. In this letter, we provide a general theory for avoidance of deforming obstacles that has the potential to be extended to a large number of applications.

II. Problem Formulation

Consider a vehicle U trying to avoid collision with a finite sized moving obstacle O with an arbitrary boundary B which is simultaneously changing its shape (See Fig. 1(a)). The boundary of the object O at times $t_0, t_1, t_2, \ldots, t_i, \ldots$, is denoted as $B_0, B_1, B_2, \ldots, B_i, \ldots$, respectively. Assume that the vehicle U is on a collision course with the object O. Now, in order to avoid collision, the evasive action to be taken by U needs to take into account not only the motion of the object O but also the fact that the boundary of O is changing with time. When O does not change shape, then the theory of collision cones provides a method to determine the cone of velocity vectors of U that would lead to collision with O [7]. Unlike other papers in the literature, the concept of collision cones proposed in [7] is applicable to arbitrarily shaped obstacles too, as long as the shape

Manuscript received September 10, 2018; accepted January 30, 2019. Date of publication February 20, 2019; date of current version March 7, 2019. This letter was recommended for publication by Associate Editor J.-M. Lien and Editor N. Amato upon evaluation of the reviewers' comments. The work of V. Sunkara and A. Chakravarthy was supported by the National Science Foundation under Grants IIS-1851817 and CNS-1446557. *(Corresponding author: Animesh Chakravarthy.)*

V. Sunkara is with the Department of Marine Science, University of Southern Mississippi, Hattiesburg, MS 39406 USA (e-mail: vishwamithra.sunkara@usm.edu).

A. Chakravarthy is with the Department of Mechanical and Aerospace Engineering, University of Texas, Arlington, TX 76019 USA (e-mail: animesh.chakravarthy@uta.edu).

D. Ghose is with the Department of Aerospace Engineering, Indian Institute of Science, Bengaluru 560012, India (e-mail: dghose@iisc.ac.in).

Digital Object Identifier 10.1109/LRA.2019.2900535

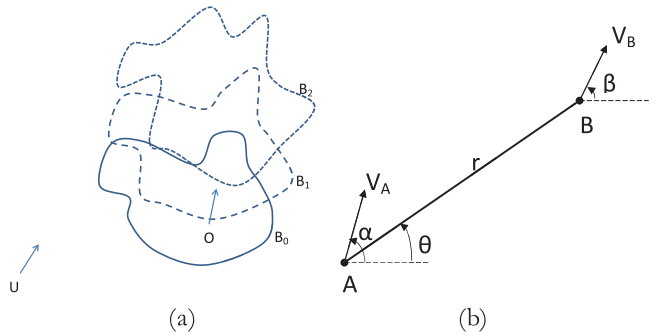

Fig. 1. (a) Schematic of a deforming object, (b) Engagement geometry between two point objects A and B.

of the obstacles do not change. In fact, it has been shown in [7] that this cone will remain invariant with time if the velocities of U and O are constant. The collision avoidance problem then reduces to the problem of determining avoidance maneuvers of the vehicle U that will pull its velocity vector out of the collision cone. However, for a deforming obstacle, although the instantaneous collision cone can be determined using the same theory, the collision cone itself is dynamic as it changes with time. Determination of the collision cone for such deforming objects and using it to design avoidance maneuvers is the subject matter of this letter.

It is worth mentioning that the same results can also be used to address an interception problem, wherein the vehicle U intends to intercept the deforming and moving object O. This can be simply done by using maneuvers that drive the velocity vector of U into the dynamic collision cone.

III. Collision Between Two Point Objects

Consider two point objects A and B (see Fig. 1(b)), moving with constant velocities, of magnitudes V_A and V_B, acting at angles α and β, respectively. Let $r(t)$ be the distance between A and B at time t, and $\theta(t)$ be the angle made by the line AB with respect to a reference. Let V_r be the relative velocity component of B with respect to A along AB and V_θ be the corresponding relative velocity component normal to AB. The expressions for these components are [13]:

$$V_r = \dot{r} = V_B \cos(\beta - \theta) - V_A \cos(\alpha - \theta) \quad (1)$$

$$V_\theta = r\dot{\theta} = V_B \sin(\beta - \theta) - V_A \sin(\alpha - \theta) \quad (2)$$

The following is a well-known result for collision:

Lemma 1: When point objects A and B move with constant velocities, the conditions $V_\theta = 0, V_r < 0$ are both necessary and sufficient conditions for collision between A and B.

Proof: See [20]. ■

IV. Collision Between a Point Object and a Deforming Object

A. Collision Conditions

Consider an engagement between a point object A and a finite-sized object B, which has the capability to deform by changing the shape of its boundary. B can represent an oil spill, or a swarm of vehicles, as schematically depicted in Fig. 2. The velocity of each point on the boundary of B is written as the vector sum

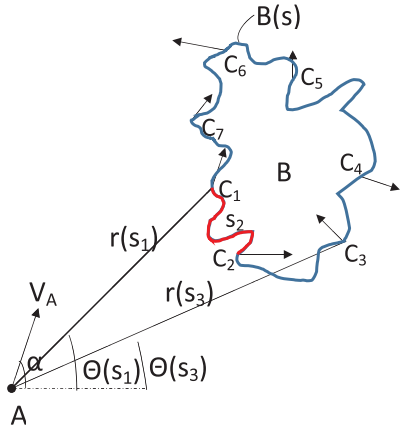

Fig. 2. Engagement between a point object A and a deforming object B.

of the individual deformation component of that point and an overall translational component. Let s be the curvilinear distance along the boundary of B, measured with respect to a reference point, and let the length of the perimeter of B be L. In Fig. 2, C_1 is the reference point and a point at a distance s from C_1 is denoted as $B(s)$ with points on the perimeter of B parametrized by $s \in [0, L]$. Let $r(s)$ be the distance between A and $B(s)$, and $\theta(s)$ be the angle made by the line joining A and $B(s)$. The points $B(s_1), B(s_2), B(s_3), ...$ are denoted by $C_1, C_2, C_3, ...$ in the figure. Let $V_B(s)$ be the magnitude of the velocity at each point $B(s)$, and $\beta(s)$ represent the corresponding direction of this velocity. Then, we can construct multiple lines AC_1, AC_2, ..., each of which have their distinct values of V_θ and V_r. We can write the relative velocity components $V_r(s) \equiv \dot{r}(s)$ and $V_\theta(s) = r(s)\dot{\theta}(s)$ as follows:

$$V_r(s) = V_B(s)\cos(\beta(s) - \theta(s)) - V_A \cos(\alpha - \theta(s)) \quad (3)$$

$$V_\theta(s) = V_B(s)\sin(\beta(s) - \theta(s)) - V_A \sin(\alpha - \theta(s)) \quad (4)$$

We then state the following lemma governing collision between A and $B(s)$.

Lemma 2: Consider a point object A and a finite object B that is simultaneously moving and deforming such that the points $B(s)$ are all moving with velocities that are constant in time. Then, A is on a collision course with B if and only if there exists at least one ray $AB(s_i)$ passing through B that has the properties $V_\theta(s_i) = 0$, $V_r(s_i) < 0$.

Proof: Follows from Lemma 1. ■

Assume that $V_B(s)$ and $\beta(s)$ both vary spatially, continuously from $s = 0$ to $s = L$. Refer Fig. 3(a), where the object B is an open chain, an example of which would be a snake robot moving on a plane. Furthermore, in Fig. 3(a), any ray AC passing through B will intersect B at exactly one point. We then have the following lemma:

Lemma 3: Let $B(s)$ be an open chain, and let the engagement geometry between A and B be such that any ray AC passing through B will intersect B at exactly one point. Then, the condition:

$$V_\theta(s = 0)V_\theta(s = L) \leq 0 \quad (5)$$

is both necessary and sufficient for there to exist exactly one $s_i \in [0, L]$ that satisfies $V_\theta(s_i) = 0$.

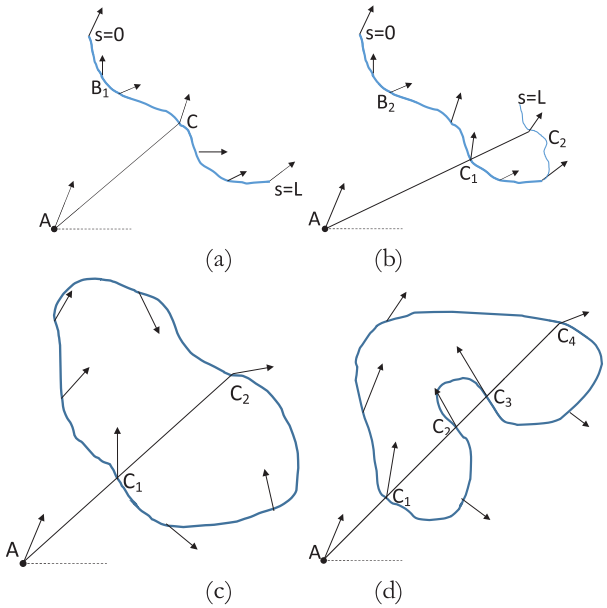

Fig. 3. Engagement geometry between a point object and (a), (b): an open chain, (c), (d): a closed chain.

Proof: Since $V_B(s)$ and $\beta(s)$ are both continuous functions of s, therefore from (3), (4), $V_\theta(s)$ also varies continuously with s. Since it is assumed that any ray from A passing through B intersects B at only one point, therefore (5) implies that the function $V_\theta(s)$ has exactly one zero crossing for $s \in [0, L]$. The converse is similarly true. ■

Next, consider the scenario in Fig. 3(b)–(d). In Fig. 3(b), $B(s)$ is still an open chain. However, there can be some rays emanating from A that will intersect $B(s)$ at more than one point. In Fig. 3(c), (d), $B(s)$ is a closed chain (which is also non-convex), examples of which could be the boundary of an oil spill or a boundary of a swarm of vehicles. In (c), any ray AC passing through $B(s)$ will intersect $B(s)$ at two points C_1 and C_2, while in (d), there are some rays emanating from A that can intersect $B(s)$ at four points. When $B(s)$ is a closed chain, then $V_\theta(s = 0) = V_\theta(s = L)$, and in such scenarios, we cannot rely on (5) to determine collision conditions. We instead use the following lemma:

Lemma 4: Let $B(s)$ be a closed chain. Then, the condition

$$\max_{s\in[0,L]} V_\theta(s) \min_{s\in[0,L]} V_\theta(s) \leq 0 \tag{6}$$

is both necessary and sufficient for there to exist at least one $s_i \in [0, L]$ that satisfies $V_\theta(s_i) = 0$.

Proof: Since $V_\theta(s)$ is a continuous function of s, therefore when (6) holds, this implies that the function $V_\theta(s)$ has at least one zero crossing. The converse is similarly true. ■

When the conditions of either Lemma 3 or Lemma 4 are satisfied, we define the collision cone as the set of heading angles of A that will cause A to collide with $B(s)$. From (4), the condition that $V_\theta(s) = 0$ is written as:

$$V_B(s)\sin(\beta(s) - \theta(s)) = V_A \sin(\alpha - \theta(s)) \tag{7}$$

From (7), for each $s \in [0, L]$, the corresponding heading angle α that will cause $V_\theta(s)$ to become zero, is as follows:

$$\alpha = \theta(s) + \sin^{-1}[(V_B(s)/V_A)\sin(\beta(s) - \theta(s))] \tag{8}$$

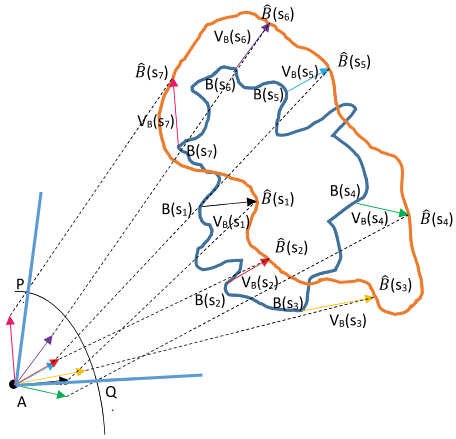

Fig. 4. Geometric interpretation of the collision cone between a point object and a finite-sized deforming object.

The collision cone is then defined as the set of α that satisfy (8) for each s, as well as $V_r(s) < 0$, that is,

$$\mathcal{C}_\alpha = \{\alpha : V_\theta(s) = 0 \cap V_r(s) < 0,\ s \in [0, L]\} \tag{9}$$

If the heading angle of A is such that it lies inside the collision cone, we can obtain an expression for the time to collision between A and $B(s)$ as follows:

$$t_m(s) = -r(s)V_r(s)/[V_r(s)^2 + V_\theta(s)^2] \tag{10}$$

where, $t_m(s)$ is always positive, since the values of $V_r(s)$ corresponding to the collision cone are all negative.

A geometric representation of the collision cone is shown in Fig. 4. The blue curve is the boundary of $B(s)$ at the current time t. Consider a few representative points $B(s_1), B(s_2), \ldots$ as shown. The vectors $V_B(s_1), V_B(s_2), \ldots$ represent the respective velocities of these points. Shift each of these velocity vectors and position them at A. For illustrative purposes, consider $V_B(s_1)$. Shift $V_B(s_1)$ to A. Then, draw a line emanating from the tip of this shifted $V_B(s_1)$ so that this line is parallel with $AB(s_1)$ and is of the same length as $AB(s_1)$. Repeat the same for the other points $B(s_2), B(s_3), \ldots$ and thus obtain the points $\hat{B}(s_2), \hat{B}(s_3), \ldots$. With A as center, draw an arc of radius equal to the speed V_A of A. Then, P and Q represent the extremal points of intersection of this arc with the rays emanating from the tip of the shifted velocity vectors of $B(s)$. The cone PAQ then represents an approximation of the collision cone. The exact collision cone would be one where the same procedure is applied to all the points on the perimeter of B. It can be seen from the figure that the extremities of the collision cone do not necessarily correspond to the extremities of the deforming object. For instance, the lower boundary of the collision cone passes through Q. If object A has a heading angle along AQ, then A will collide with $B(s_4)$ even though $B(s_3)$ lies to the right of $B(s_4)$ (from the viewpoint of A).

B. Guidance Laws for Collision Avoidance

We now determine guidance laws that will ensure that A avoids a collision with B. Let the acceleration magnitude of A be a_A, applied at an angle δ_A. Then, the kinematics of the engagement between A and $B(s)$ are represented by the following

equations, valid for all $s \in [0, L]$:

$$\dot{r}(s) = V_r(s) \tag{11}$$

$$\dot{\theta}(s) = V_\theta(s)/r(s) \tag{12}$$

$$\dot{V}_\theta(s) = -V_\theta(s)V_r(s)/r(s) - a_A \sin(\delta_A - \theta(s)) \tag{13}$$

$$\dot{V}_r(s) = V_\theta(s)^2/r(s) - a_A \cos(\delta_A - \theta(s)) \tag{14}$$

Define a set S as follows:

$$S = \{s \in [0, L] : V_r(s) < 0\} \tag{15}$$

An avoidance acceleration for A is one that drives the maximum value of $V_\theta(s)$ that lies in the set S to zero. This will physically correspond to A grazing the surface of B. To determine such a collision avoidance law, define a candidate Lyapunov function as:

$$Z = (1/2)[\max_{s \in S} V_\theta(s)]^2 \tag{16}$$

The time derivative of the Lyapunov function along the trajectories of the system (11)–(14) is:

$$\begin{aligned}\dot{Z} &= m[V_\theta(s)] \\ &\times \left[\frac{\partial m[V_\theta(s)]}{\partial r(s)} \ \frac{\partial m[V_\theta(s)]}{\partial \theta(s)} \ \frac{\partial m[V_\theta(s)]}{\partial V_\theta(s)} \ \frac{\partial m[V_\theta(s)]}{\partial V_r(s)} \right] \\ &\times \left[\dot{r}(s) \ \dot{\theta}(s) \ \dot{V}_\theta(s) \ \dot{V}_r(s) \right]^T \end{aligned} \tag{17}$$

In the above equation, $m[V_\theta(s)] \equiv \max_{s \in S} V_\theta(s)$, and it is understood that $\partial(.)/\partial r(s)$ is a vector of the form: $\partial(.)/\partial r(s) = \left[\partial(.)/\partial r(s_1) \ \partial(.)/\partial r(s_2) \cdots \right]$. Expressions for the vector quantities $\partial(.)/\partial\theta(s)$, $\partial(.)/\partial V_\theta(s)$, $\partial(.)/\partial V_r(s)$ are similarly written. Defining

$$\bar{s} \equiv \arg\max_{s \in S} V_\theta(s) \tag{18}$$

the time derivative $\dot{Z}$ can be written as:

$$\begin{aligned}\dot{Z} &= V_\theta(\bar{s})\dot{V}_\theta(\bar{s}) \\ &= V_\theta(\bar{s})[-V_\theta(\bar{s})V_r(\bar{s})/r(\bar{s}) - a_A \sin(\delta_A - \theta(\bar{s}))] \end{aligned} \tag{19}$$

By choosing a guidance law of the form:

$$a_A = V_\theta(\bar{s})[K - V_r(\bar{s})/r(\bar{s})]/[\sin(\delta_A - \theta(\bar{s}))] \tag{20}$$

with $K > 0$, it can be ensured that the Lyapunov function Z has a negative definite time derivative, and follows the dynamics $\dot{Z} = -2KZ$. With guidance law (20), $m[V_\theta(s)]$ will asymptotically decay to zero, and this will cause the point object A to graze the surface of the deforming object B. Eqn (20) thus guarantees that collision avoidance is achieved, provided the gain K is sufficiently large to ensure that Z decays to a small number ϵ before time $t_m(\bar{s})$.

We note that depending on the shape of the object B, there can be discontinuities in the value of $\bar{s}$, as the engagement evolves in time. For the sake of simplicity, the analysis involving such discontinuities is omitted in this letter.

When the translational and/or deformation velocities of the object $B(s)$ vary with time, that is, $B(s)$ has an acceleration of magnitude $a_B(s)$, acting at angles given by $\delta_B(s)$, then (13) and (14) assume the form:

$$\dot{V}_\theta(s) = f_\theta + a_B(s)\sin(\delta_B(s) - \theta(s)) \tag{21}$$

$$\dot{V}_r(s) = f_r + a_B(s)\cos(\delta_B(s) - \theta(s)) \tag{22}$$

where f_θ and f_r are the terms on the right hand sides of (13) and (14) respectively. Differentiating the Lyapunov function (16) along the trajectories of (11)–(12), (21)–(22) and substituting (20), we obtain:

$$\dot{Z} = -2KZ + a_B(\bar{s})V_\theta(\bar{s})\sin(\delta_B(\bar{s}) - \theta(\bar{s})) \tag{23}$$

From (23), it is evident that as long as the acceleration law (20) uses a K that is large enough to keep the right hand side of (23) negative definite, and furthermore, as $Z \to 0$, the deformation of $B(s)$ is such that $a_B(\bar{s}) \to 0$, then the law (20) will guarantee that A avoids collision with B.

V. Collision Between a Circular Object and a Deforming Object

A. Collision Conditions

In this subsection, we first consider the collision conditions between a point and a circle, and then show how it can be used to determine the collision condition between a circle and a deforming object. Consider an engagement between a point and a circle (which is non-deforming), of radius R. As demonstrated in [7], we can define a collision cone function y for this engagement, as follows:

$$y = r^2V_\theta^2/[V_\theta^2 + V_r^2] - R^2 \tag{24}$$

where, r is the distance between the point and the center of the circle, and V_r, V_θ represent the relative velocity components of this line. The quantity y is essentially a function of the miss-distance between the point object and the center of the circle, at the instant of closest approach. We have the following:

Lemma 5: Consider an engagement between a point object and a circular object, where both objects move with constant velocities. Then, the conditions $y < 0$, $V_r < 0$ are both necessary and sufficient for occurrence of a collision.

Proof: See [7], where it is demonstrated that the conditions $y < 0$, $V_r < 0$, physically correspond to the scenario that the relative velocity vector lies inside the collision cone. ■

Now, consider an engagement between a circular object A (which is non-deforming) and a deforming object B, as shown in Fig. 5. Let P be the center of the circle A. For every possible line that can be drawn from P to the boundary $B(s)$, let $r(s)$ be the length and $\theta(s)$ be the bearing angle. Similarly, let $V_r(s)$ and $V_\theta(s)$ represent the relative velocity components of each such line. We can use (24) to define a function $y(s)$:

$$y(s) = r(s)^2V_\theta(s)^2/[V_\theta(s)^2 + V_r(s)^2] - R^2 \tag{25}$$

We then have the following:

Lemma 6: Let A and $B(s)$ move with constant (in time) velocity vectors $\vec{V}_A$ and $\vec{V}_B(s)$, respectively. Then, A is on a collision course with $B(s)$ if and only if there exist some $s \in [0, L]$ that satisfy $y(s) < 0$ and $V_r(s) < 0$.

Proof: If $y(s) < 0$ and $V_r(s) < 0$ for some $\hat{s} \in [0, L]$, then the circle A is on a collision course with the point(s) $\hat{s}$ on $B(s)$. The converse is also true. The proof then follows. ■

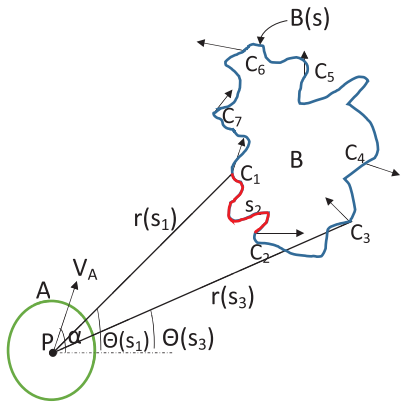

Fig. 5. Engagement between a circular object A and deforming object B.

The function $y(s)$ can then be used to define the collision cone between A and $B(s)$ as follows:

$$\mathcal{C}_\alpha = \{\alpha : y(s) < 0 \cap V_r(s) < 0, s \in [0, L]\} \tag{26}$$

B. Guidance Laws for Collision Avoidance

An avoidance acceleration for A is one that drives the minimum value of $y(s)$ that lies in the set S (defined in (15)) to zero. This will physically correspond to A grazing the surface of B. To determine such an acceleration law, define a candidate Lyapunov function as:

$$Z = (1/2)[\min_{s\in S} y(s)]^2 \tag{27}$$

The time derivative of the Lyapunov function along the trajectories of the system (11)–(14) is:

$$\begin{aligned}\dot{Z} = {} & m[y(s)] \\ & \times \left[\frac{\partial m[y(s)]}{\partial r(s)} \;\; \frac{\partial m[y(s)]}{\partial \theta(s)} \;\; \frac{\partial m[y(s)]}{\partial V_\theta(s)} \;\; \frac{\partial m[y(s)]}{\partial V_r(s)}\right] \\ & \times \left[\dot{r}(s) \;\; \dot{\theta}(s) \;\; \dot{V}_\theta(s) \;\; \dot{V}_r(s)\right]^T\end{aligned} \tag{28}$$

where, for the sake of brevity, we have employed the notation

$$m[y(s)] = \min_{s\in S} y(s) \tag{29}$$

Defining $\underline{s} \equiv \arg\min_{s\in S} y(s)$, we have $\dot{Z} = y(\underline{s})\dot{y}(\underline{s})$ as:

$$\begin{aligned}\dot{Z} = {} & -2y(\underline{s})r(\underline{s})^2 V_\theta(\underline{s})V_r(\underline{s})a_A[V_r(\underline{s})\sin(\delta_A - \theta(\underline{s})) \\ & - V_\theta(\underline{s})\cos(\delta_A - \theta(\underline{s}))]/[V_r(\underline{s})^2 + V_\theta(\underline{s})^2]^2\end{aligned} \tag{30}$$

By choosing a guidance law of the form:

$$\begin{aligned}a_A = {} & -0.5Ky(\underline{s})[V_\theta(\underline{s})^2 + V_r(\underline{s})^2]^2/\big[r(\underline{s})^2 V_\theta(\underline{s})V_r(\underline{s}) \\ & \{-V_r(\underline{s})\sin(\delta_A - \theta(\underline{s})) + V_\theta(\underline{s})\cos(\delta_A - \theta(\underline{s}))\}\big]\end{aligned} \tag{31}$$

where $K > 0$, it can be ensured that the Lyapunov function Z follows the dynamics $\dot{Z} = -2KZ$, and this will cause $m[y(s)]$ to exponentially go to zero. The guidance law (31) thus guarantees that collision avoidance is achieved, provided K is large enough to ensure Z decays to ϵ (where ϵ is a small number) before time $t_m(\underline{s})$.

When B has an acceleration $a_B(s)$, acting at an angle $\delta_B(s)$, then after differentiating (27) along (11), (12), (21), (22) and substituting (31), the resulting equation is the same as (23). Similar to the comments made after (23), as long as the value of K employed in (31) is such that it ensures that $\dot{Z}$ remains negative definite and Z is driven to zero before the instant of closest approach occurs, collision between A and B will be avoided.

Implementation: From an implementation standpoint, we assume that a sensor tracks the boundary of the deforming object. The type of sensor would depend on the environment. For example, in the case when the deforming object B is either an oil spill, or a vehicle swarm on a water surface, the sensor could potentially be a vision sensor located on the hull of a ship (or on an elevated point on the ship), or on one or more airborne UAVs looking down on this deforming entity. In the case when the deforming object B is a snake-like robot moving on the ground, then the sensor could potentially be a lidar placed on object A, which sweeps back and forth across the periphery of B. In either case, the sensor information is used to obtain the values of $V_B(s)$, $\beta(s)$, $\theta(s)$, $r(s)$.

The algorithm for the collision avoidance law for the engagement of Fig. 5 is given below:

Algorithm A1 Let L Represent the Circumference of B at Time t. At Time t:

a) Use sensor information to determine L and $V_B(s)$, $\beta(s)$, $\theta(s)$, $r(s)$ for $s \in [0, L]$.
b) Use the above to compute $V_r(s)$, $V_\theta(s)$, and $y(s)$, for $s \in [0, L]$, using (3), (4) and (25), respectively.
c) Determine the set $S \subset [0, L]$, for which $V_r(s) < 0$.
d) Determine value of $\underline{s} \in S$, at which minimum $y(s)$ occurs. If $y(\underline{s}) < 0$, apply acceleration (31), else, continue with original velocity.
e) Update time to $t + \Delta t$, and go to (a).

The above algorithm requires the determination of the minimum of $y(s)$, as well as $\underline{s}$. This involves a 1-dimensional search, and any standard search method may be used.

C. Merging Objects

There can be scenarios wherein two or more deforming objects may merge into a single deforming object. An example is when multiple oil spills on a water surface merge together. Consider two deforming objects B_1 and B_2, that subsequently merge. The collision avoidance algorithm is given in Algorithm A2:

Stability of the collision avoidance law continues to hold even in the case of merging objects. In the case of two merging deforming objects, the Lyapunov function (27) needs to be modified so as to take the minimum of $y(s)$ over the boundary points of both deforming objects. After the deforming objects merge, the minimum of $y(s)$ is taken over the boundary of the single merged object. The rest of the steps are conceptually similar to those shown in (28)–(31). We omit the detailed proof due to space constraints.

Algorithm A2 Let L_1 and L_2 Represent the Circumferences of B_1 and B_2, at time t. At Time t:

a) Use sensor information to determine L_1, L_2, $V_B(s^1)$, $\beta(s^1)$, $\theta(s^1)$, $r(s^1)$ for $s^1 \in [0, L_1]$, and also $V_B(s^2)$, $\beta(s^2)$, $\theta(s^2)$, $r(s^2)$ for $s^2 \in [0, L_2]$.
b) Use the above to compute $V_r(s^1)$, $V_\theta(s^1)$, and $y(s^1)$, for $s^1 \in [0, L_1]$, and $V_r(s^2)$, $V_\theta(s^2)$, $y(s^2)$, for $s^2 \in [0, L_2]$ using (3), (4) and (25).
c) Find the set $S_1 \subset [0, L_1]$, for which $V_r(s^1) < 0$ for $s^1 \in S_1$, and $S_2 \subset [0, L_2]$, for which $V_r(s^2) < 0$ for $s^2 \in S_2$.
d) Determine value of $\underline{s}^1 \in S_1$, at which minimum $y(s^1)$ occurs, and $\underline{s}_2 \in S_2$, at which minimum $y(s^2)$ occurs. From these, determine $y_{min} \equiv \min(y(\underline{s}^1), y(\underline{s}^2))$. If $y_{min} < 0$, apply acceleration (31), else, continue with original velocity.
e) Update time to $t + \Delta t$. If B_1 and B_2 are still disjoint, go to (a). If B_1 and B_2 have merged, go to (a) of A1.

VI. Collision Between an Arbitrarily Shaped Object and a Deforming Object

A. Collision Conditions

First, consider an engagement between a point object and an arbitrarily shaped object (which is non-deforming). We can construct a pair of lines that emanate from the point and are tangents to the arbitrarily shaped object. In general, there can be multiple such tangents. We consider the specific pair of tangents that subtend the largest angle at the point object. As shown in [7], we can define a collision cone function y between the point and the arbitrarily shaped object as:

$$y = V_\theta^2/[V_\theta^2 + V_r^2] - \sin^2(\psi/2) \tag{32}$$

where, ψ is the angle subtended by the above pair of tangents at the point object, and V_r, V_θ represent the relative velocity components of the line which is the angular bisector of the sector formed by the pair of tangents.

Lemma 7: Consider an engagement between a point object and an arbitrarily shaped object, where both objects move with constant velocities. Then, if the engagement is such that $\psi < \pi$, the conditions $y < 0$, $V_r < 0$ are both necessary and sufficient for a collision to occur between the objects.

Proof: See [7].

We now use the above result to define the collision cone between an arbitrarily shaped object A (which is non-deforming) and a deforming object B. The engagement is shown in Fig. 6. From each point $B(s)$ on the boundary of B, construct tangents to A, and consider the pair of tangents that subtend the largest angle at $B(s)$. For instance, in Fig. 6, the tangents to A emanating from C_1 are the lines C_1P_{C1} and C_1Q_{C1} and the angle between these tangents is $\psi(s_1)$. Similarly, the tangents to A emanating from C_3 are C_3P_{C3} and C_3Q_{C3}, and the angle between them is $\psi(s_3)$. We can thus define a function $\psi(s)$.

The quantities $V_r(s_1)$ and $V_\theta(s_1)$ represent the relative velocity components of the angular bisector of the sector $P_{C1}C_1Q_{C1}$. Similarly, $V_r(s_3)$ and $V_\theta(s_3)$ represent the relative velocity components of the angular bisector of the sector $P_{C3}C_3Q_{C3}$. In this way, we can define functions $V_\theta(s)$ and $V_r(s)$. Eventually, we

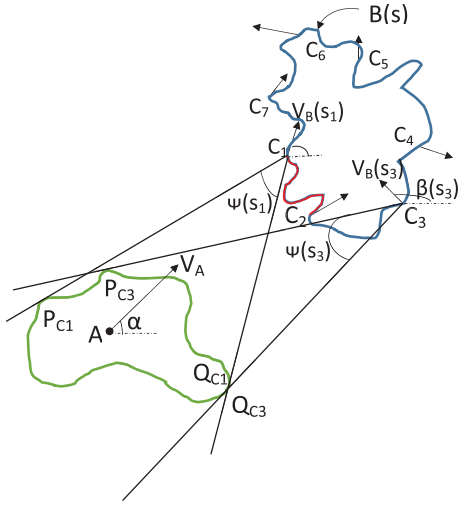

Fig. 6. Engagement between arbitrary object A and deforming object B.

can use the functions $\psi(s)$, $V_\theta(s)$ and $V_r(s)$ to define a function $y(s)$ as follows:

$$y(s) = V_\theta(s)^2/[V_\theta(s)^2 + V_r(s)^2] - \sin^2[\psi(s)/2] \tag{33}$$

Using the above definitions of $y(s)$ and $V_r(s)$, we can state the following Lemma:

Lemma 8: Let A be an arbitrarily shaped object moving with a constant velocity $\vec{V}_A$ and B be a deforming object whose boundary $B(s)$ is moving with velocity $\vec{V}_B(s)$, where $\vec{V}_B(s)$ is constant in time, for each s. Furthermore, assume the engagement is such that $\psi(s) < \pi, \forall s \in [0, L]$. Then, A is on a collision course with $B(s)$ if and only if there exist some $s \in [0, L]$ that satisfy $y(s) < 0$ and $V_r(s) < 0$.

Proof: If $y(s) < 0$ and $V_r(s) < 0$ for some $\hat{s} \in [0, L]$, then the arbitrarily shaped object A is on a collision course with the point(s) $\hat{s}$ on the deforming object $B(s)$. The converse is similarly true. The proof then follows.

The collision cone between A and $B(s)$ is defined as in (26), where $y(s)$ is as defined in (33) and $V_r(s)$ is defined as discussed above.

B. Guidance Laws for Collision Avoidance

An avoidance acceleration for A is one that drives the minimum value of $y(s)$ to zero. By defining a Lyapunov function as given in (27), with $y(s)$ defined as in (33), and performing a series of steps similar to (30), we can obtain a guidance law for collision avoidance between the arbitrary object A and the deforming object $B(s)$ as follows:

$$\begin{aligned} a_A = \Big[& -Ky(\underline{s})(V_r(\underline{s})^2 + V_\theta(\underline{s})^2)^2 \\ & + 2(V_r(\underline{s})^2 + V_\theta(\underline{s})^2)V_\theta(\underline{s})^2 \mathrm{cosec}^2(\psi(\underline{s})/2) \\ & (V_r(\underline{s})\dot{\theta}(\underline{s})/V_\theta(\underline{s}) + \cot(\psi(\underline{s})/2)(\dot{\psi}(\underline{s})/2)\Big]/ \\ & \Big[2V_r(\underline{s})V_\theta(\underline{s})\mathrm{cosec}^2(\psi(\underline{s})/2)(-V_r(\underline{s})\sin(\delta - \theta(\underline{s})) \\ & + V_\theta(\underline{s})\cos(\delta - \theta(\underline{s}))\Big] \end{aligned} \tag{34}$$

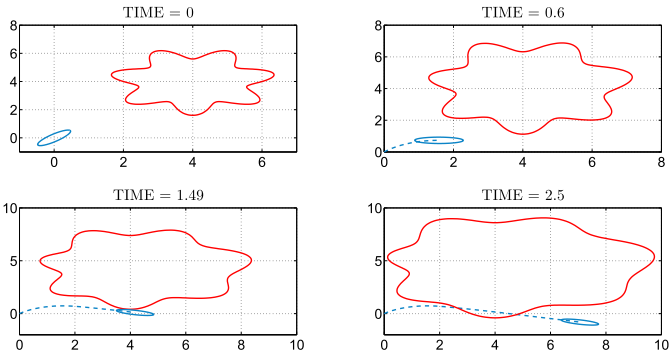

Fig. 7. Spatial trajectories of object A and oil spill B.

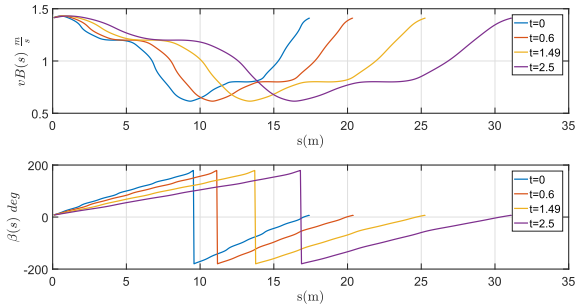

Fig. 8. Velocity distribution of $B(s)$ at several instants in time.

The above acceleration will ensure that $m[y(s)]$ is driven to zero, and this will cause A to graze B at its periphery.

In the case when B is accelerating, substituting (34) in (28) (evaluated along (11), (12), (21), (22)) leads to (23), and a similar condition on the gain K (as made in the previous section discussing the engagement of Fig. 5) will ensure that A avoids B. The algorithm to implement the collision avoidance laws for the scenario of Fig. 6 would be similar to that shown in Section V for Fig. 5, with the following changes for A1: In step (a), in lieu of $r(s)$, compute $\psi(s)$, using available algorithms to compute the conical hull of an object, such as [21], for example. In step (b), compute $y(s)$ using (33). In step (d), compute the acceleration using (34). The counterpart of the A2 algorithm in Section V can be written similarly.

VII. Simulations

We present simulations that demonstrate the working of the guidance laws developed above. We consider an engagement between an arbitrarily shaped object A and a deforming object B. A is taken to be an oval shape (it may represent an autonomous boat on an ocean), while B represents the boundary of an oil spill whose shape is changing with time. The points $s_1, s_2, \ldots$ on the boundary of $B(s)$ are moving with distinct velocities $V_B(s_1), V_B(s_2), \ldots$. The speed distribution $V_B(s)$ and heading angle distribution $\beta(s)$ are given in Fig. 8. The influence of this speed distribution is that B follows a translation and deformation trajectory as shown in Fig. 7, from which it is evident that the deformations cause the length L of $B(s)$ to increase with time. Accordingly, the domain of the horizontal axis in Fig. 8 is small at $t = 0$, and then becomes progressively larger with time.

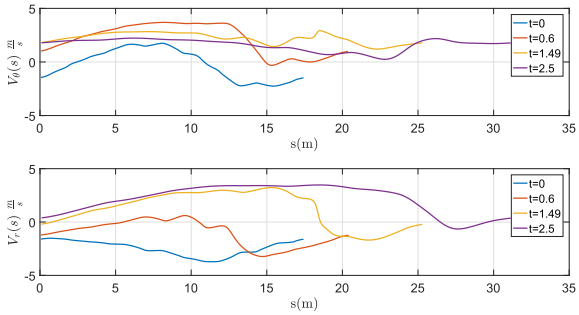

Fig. 9. Relative velocity functions $V_r(s)$ and $V_\theta(s)$ at several times.

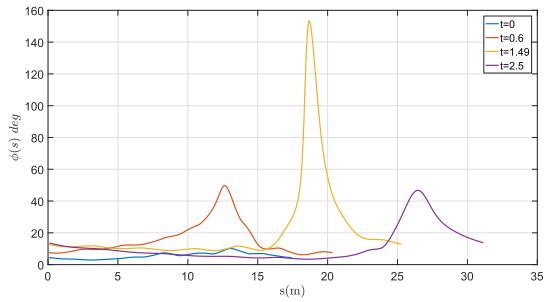

Fig. 10. Angle function $\psi(s)$ at several instants in time.

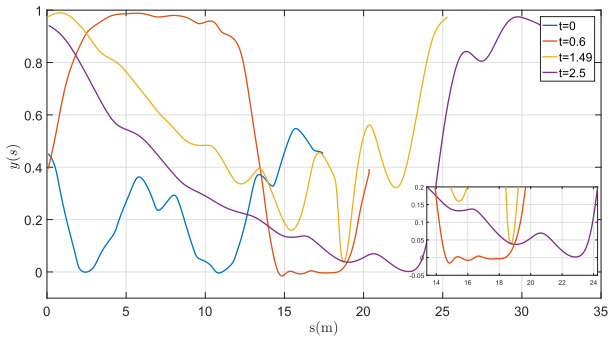

Fig. 11. Collision cone function $y(s)$ at several instants in time.

A moves with a constant speed of 5 m/sec, and its initial heading angle is 45^0, which lies inside the collision cone. If A continues to move with its initial velocity vector, it would collide with B. Using the guidance law (34), A is able to drive its velocity vector out of the collision cone and avert collision, as evident from Fig. 7, where it is seen that A grazes the circumference of the oil spill B at $t = 1.49$ sec. The relative velocity functions $V_\theta(s)$ and $V_r(s)$ are shown in Fig. 9, as time snapshots at several instants in time. The angle function $\psi(s)$ is shown at the same times in Fig. 10. Using $V_\theta(s)$, $V_r(s)$ and $\psi(s)$, the resulting $y(s)$ is shown in Fig. 11. From Fig. 11, at $t = 0$, the $y(s)$ function is negative for some s, and $V_r(s)$ is negative for almost all s (Fig. 9). Under the influence of the guidance laws, the function $y(s)$ is driven to be non-negative for all s. Fig. 12 shows the acceleration profile. This acceleration was applied normal to the velocity vector of A, and therefore changed the heading angle of A with no change in speed. The change in the heading angle of A is also shown in Fig. 12.

In a second example, Fig. 13 shows how the guidance laws can ensure that the autonomous boat successfully avoids collision with two oil spills, as they merge. In a third example, consider

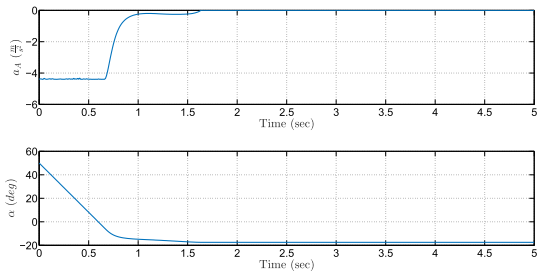

Fig. 12. Applied acceleration and heading angle of object A.

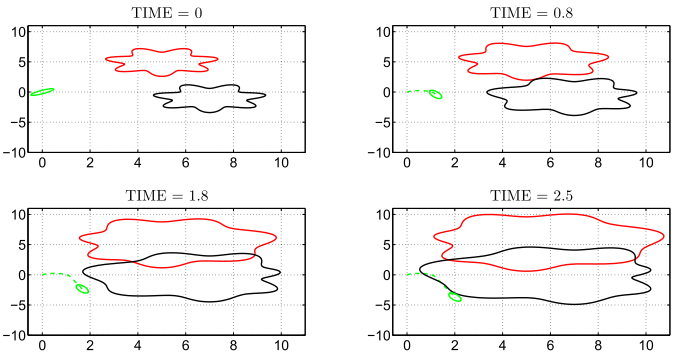

Fig. 13. Spatial trajectories of object A and two merging oil spills.

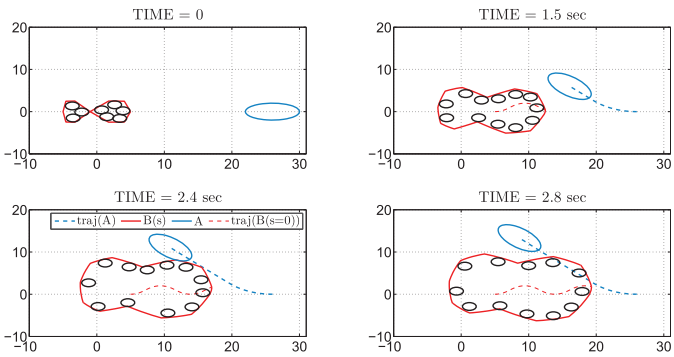

Fig. 14. Spatial trajectories of object A and shape-changing swarm B.

the object A navigating an environment containing a swarm of vehicles, moving in a non-rigid formation. The boundary of the swarm B changes with time as shown in Fig. 14. The initial conditions are such that A is on a collision course with B. Using the guidance laws developed, A avoids colliding with B and at time $t = 2.4$ sec, A grazes the boundary B as seen in Fig. 14.

VIII. Conclusions

The problem of collision avoidance with deformable objects is considered. Examples of objects that have the ability to deform include snake robots, boundaries of oil spills and boundaries of vehicle swarms. We develop the notion of a collision cone associated with such deformable objects. We first develop the collision cone between a point object and a deformable object, and subsequently extend it to the case of an engagement between a circular object and a deforming object. We finally demonstrate the collision cone between an arbitrarily shaped object and a deforming object. For each of these cases, the collision cone functions are embedded in a Lyapunov framework, which is used to develop analytical expressions of nonlinear guidance laws to enable collision avoidance. Simulations are presented to validate the theory. Treatment of scenarios that involve the presence of discontinuities at the boundaries of deforming objects is a promising avenue for further work.

References

[1] D. Trivedi, C. D. Rahn, W. M. Kier, and I. D. Walker, "Soft robotics: Biological inspiration, state of the art and future research," *Appl. Bionics Biomechanics*, vol. 5, no. 3, pp. 99–117, 2008.

[2] S. Kim, C. Laschi, and B. Trimmer, "Soft robotics: A bio-inspired evolution in robotics," *Trends Biotechnology*, vol. 31, no. 5, pp. 287–294, May 2013.

[3] A. S. Matveev, C. Wang, and A. V. Savkin, "Real-time navigation of mobile robots in problems of border patrolling and avoiding collisions with moving and deforming obstacles," *Robot. Auton. Syst.*, vol. 60, no. 6, pp. 769–788, Jun. 2012.

[4] A. S. Matveev, M. C. Hoy, and A. V. Savkin, "A globally converging algorithm for reactive robot navigation among moving and deforming obstacles," *Automatica*, vol. 54, pp. 292–304, Apr. 2015.

[5] B. Frank, C. Stachniss, R. Schmedding, M. Teschner, and W. Burgard, "Real-world robot navigation amongst deformable obstacles," in *Proc. Int. Conf. Robot. Autom.*, 2009, pp. 1649–1654.

[6] K. L. Chaudhary and D. Ghose, "Path planning in dynamic environments with deforming obstacles using collision cones," in *Proc. Indian Control Conf.*, Guwahati, India, 2017, pp. 87–92.

[7] A. Chakravarthy and D. Ghose, "Obstacle avoidance in a dynamic environment: A collision cone approach," *IEEE Trans. Syst., Man, Cybern. A, Syst. Humans*, vol. 28, no. 5, pp. 562–574, Sep. 1998.

[8] A. Ferrara and C. Vecchio, "Second order sliding mode control of vehicles with distributed collision avoidance capabilities," *Mechatronics*, vol. 19, pp. 471–477, 2009.

[9] J. Goss, R. Rajvanshi, and K. Subbarao, "Aircraft conflict detection and resolution using mixed gometric and collision cone approaches," in *Proc. AIAA Guid., Navigation, Control Conf. Exhibit*, Providence, RI, USA, Aug. 2004, Paper No. AIAA 2004-4879.

[10] Y. Watanabe, A. J. Calise, E. N. Johnson, and J. H. Evers, "Minimum-effort guidance for vision-based collision avoidance," in *Proc. AIAA Atmospheric Flight Mechanics Conf. Exhibit*, Keystone, CO, USA, Aug. 2006, Paper No. AIAA 2006-6641.

[11] B. Gopalakrishnan, A. K. Singh, and K. M. Krishna, "Time scaled collision cone based trajectory optimization approach for reactive planning in dynamic environments," in *Proc. IEEE/RSJ Int. Conf. Intell. Robots Syst.*, Chicago, IL, USA, 2014, pp. 4169–4176.

[12] N. Brace *et al.*, "Using collision cones to assess biological deconfliction methods," *J. Roy. Soc. Interface*, vol. 13, no. 122, pp. 1–8, 2016.

[13] A. Chakravarthy and D. Ghose, "Collision cones for quadric surfaces," *IEEE Trans. Robot.*, vol. 27, no. 6, pp. 1159–1166, Dec. 2011.

[14] A. Chakravarthy and D. Ghose, "Generalization of the collision cone approach for motion safety in 3-dimensional environments," *Auton. Robots*, vol. 32, no. 3, pp. 243–266, Apr. 2012.

[15] A. Chakravarthy and D. Ghose, "Collision cones for quadric surfaces in $n-$dimensions," *IEEE Robot. Autom. Lett.*, vol. 3, no. 1, pp. 604–611, Jan. 2018.

[16] A. Chakravarthy and D. Ghose, "Guidance laws for precision 3-dimensional maneuvers through orifices using safe-passage cones," *J. Guid. Control Dyn.*, vol. 39, no. 6, pp. 1325–1341, 2016.

[17] L. P. Tychonievich, D. Zaret, R. Mantegna, R. Evans, E. Muehle, and S. Martin, "A maneuvering-board approach to path planning with moving obstacles," in *Proc. Int. Joint Conf. Artif. Intell.*, 1989, pp. 1017–1021.

[18] P. Fiorini and Z. Shiller, "Motion planning in dynamic environments using velocity obstacles," *Int. J. Robot. Res.*, vol. 17, no. 7, pp. 760–772, 1998.

[19] B. Damas and J. Santos-Victor, "Avoiding moving obstacles: The forbidden velocity map," in *Proc. IEEE/RSJ Int. Conf. Intell. Robots Syst.*, 2009, pp. 4393–4398.

[20] C. Lin, *Modern Navigation, Guidance and Control Processing*. Englewood Cliffs, NJ, USA: Prentice-Hall, 1991.

[21] A. Kumar, V. Sindhwani, and P. Kambadur, "Fast conical hull algorithms for near-separable non-negative matrix factorization," in *Proc. Int. Conf. Mach. Learn.*, 2013, vol. 28, pp. 231–239.